THE ASTROPHYSICAL JOURNAL 242:756–764, 1980 December 1

AXIAL ROTATION, TANGLED MAGNETIC FIELDS, AND THEORETICAL MODELS OF VERY MASSIVE STARS

RICHARD STOTHERS
NASA Institute for Space Studies, Goddard Space Flight Center
Received 1980 April 21; accepted 1980 June 3

ABSTRACT

A simple method of computing theoretical models of very massive stars endowed with fast axial rotation and tangled magnetic fields is described and used in the present paper. Both of the two perturbing (nongravitational) forces induce changes in the luminosity and radius that are studied as functions of zero-age chemical composition, opacity, and evolutionary state of the interior. The central condensation of the star is found to have a significant influence on shifts of the upper main-sequence band in the H-R diagram if the perturbing force is concentrated in the stellar envelope (but not if the perturbing force is distributed so as to be approximately proportional to gravity everywhere); the layers of the envelope that contribute most heavily to the central condensation lie approximately at a radius fraction of $r/R = 0.5$. It is shown that fast uniform rotation and intense envelope magnetic fields lead to probably the largest possible shifts of the main-sequence band in the H-R diagram that rotation and magnetic fields can induce. These displacements are, however, too small to account for the total width of the observed main-sequence band at luminosities brighter than $\log (L/L_{\odot}) = 4.5$.

Subject headings: stars: interiors — stars: magnetic — stars: massive — stars: rotation

I. INTRODUCTION

Evolutionary studies of rapidly rotating stars on the upper main sequence have so far been concerned largely with stars with masses of 10 $M_{\odot}$ and less (Sackmann and Anand 1970; Strittmatter, Robertson, and Faulkner 1970; Kippenhahn, Meyer-Hofmeister, and Thomas 1970; Meyer-Hofmeister and Thomas 1970; Musylev, Tutukov, and Chevalier 1970; Meyer-Hofmeister 1972; Gredley and Borra 1972; Tuominen and Musylev 1974; Endal and Sofia 1976, 1978, 1979). It is of obvious theoretical interest to extend the study of these stars to higher masses, for which the only studies thus far published, with one minor exception (Musylev 1972), refer to unevolved stars (Mark 1968; Jackson 1970*b*; Sackmann and Anand 1970; Sackmann 1970; Bodenheimer and Ostriker 1970; Bodenheimer 1971; Monaghan and Smart 1971; Harris and Clement 1971; Whelan, Papaloizou, and Smith 1971; Papaloizou and Whelan 1973; Stothers 1974; Clement 1979). An additional motivation is provided by the following two observational facts. First, many O-type stars are observed to be fast rotators (Slettebak 1956; Balona 1975; Conti and Ebbets 1977; Ebbets 1979), although precise values for their rotational velocities have not yet been determined in most cases. Second, the empirical main-sequence band as displayed in the H-R diagram exhibits an enormous width for O-type stars, which extends even into the region of bright B-type supergiants (Kopylov 1959; Andrews 1968; Stothers 1972; Humphreys and Davidson 1979). The question therefore arises whether rotational effects, which are known to expand stellar envelopes, may account for this extraordinary widening.

Another possible agent having qualitatively the same effect as rotation is a severely tangled magnetic field. Although it is not yet feasible to measure the magnetic fields of O stars (whose spectral lines are significantly broadened by rotation and macroturbulence), magnetic fields ought to be present in some strength as a result of the amplification of primordial seed fields during the pre–main-sequence collapse phase. Furthermore, convection and rotation may be assumed to have tangled the magnetic field lines to a large extent. Somewhat surprisingly, only a few models of upper-main-sequence stars with tangled magnetic fields have been published so far (Trasco 1970; Tutukov and Ruben 1974; Dudorov 1974; Stothers 1979).

The purpose of the present paper is to determine the extent to which axial rotation and tangled magnetic fields can affect the location of very massive main-sequence stars in the H-R diagram. It will be demonstrated in § II that certain simplifying conditions prevailing in the interiors of very massive stars permit their structure at any specified stage of evolution on the main sequence to be computed without recourse to laborious calculations of detailed evolutionary tracks. Consequently, the predicted main-sequence bands for rotating and magnetic stars of high mass can easily be computed. The results of these calculations are given in §§ III and IV, and a comparison with observations is presented in § V.

II. UNPERTURBED STAR MODELS

A brief description of the structure of nonrotating, nonmagnetic stars of high mass will be given here for the purpose of orientation.

TABLE 1

NONROTATING, NONMAGNETIC STAR MODELS

Stage	$M/M_\odot$	$\log (L/L_\odot)$	$\log (R/R_\odot)$	$\log T_e$	$\log T_c$	$\log \rho_c$	β_c	$\rho_c/\langle\rho\rangle$	X_c
ZAMS.....	15	4.261	0.689	4.484	7.509	0.735	0.898	30	0.739
	30	5.047	0.850	4.600	7.561	0.499	0.782	27	0.739
	60	5.687	1.009	4.680	7.600	0.312	0.640	26	0.739
	120	6.213	1.171	4.731	7.629	0.153	0.501	27	0.739
TAMS.....	15	4.557	0.983	4.411	7.630	1.003	0.771	423	0.040
	30	5.368	1.238	4.486	7.690	0.798	0.576	768	0.026
	60	5.947	1.457	4.522	7.729	0.642	0.417	1217	0.019
	120	6.397	1.656	4.535	7.753	0.495	0.302	1713	0.018

According to the prevailing view, a normal star of high mass lying on the zero-age main sequence (ZAMS) is composed of a radiative envelope and a convective core. By the time evolution has carried the star to its coolest effective temperature during the phase of core hydrogen burning (the TAMS stage), the convective core, now almost devoid of hydrogen, has shrunk down to a small fraction of its original mass. Layers that were formerly inside the convective core comprise an intermediate zone containing a gradient of hydrogen and helium.

The present simplification in computing these evolved models is to regard the inhomogeneous zone, which is at least partly convectively unstable, as being completely semiconvective in the sense originally proposed by Schwarzschild and Härm (1958). It then follows from their work that, once the central hydrogen abundance X_c is specified, the whole stellar structure is uniquely determined without regard to the prior evolutionary history, because the hydrogen abundance at each layer of the inhomogeneous zone is simply adjusted to satisfy the condition of convective neutrality,

$$\nabla_{\rm rad} = \nabla_{\rm ad} \,. \tag{1}$$

Most other treatments of the inhomogeneous zone have been found to lead to very similar structures for the star (Stothers 1972; Schlesinger 1975).

In the present work, stellar models for the ZAMS and TAMS stages have been computed by using essentially the same physical input data as in an earlier paper (Stothers 1972). The initial (hydrogen, metals) abundance has been taken to be $(X_e, Z_e) = (0.739, 0.021)$; Cox-Stewart opacities have been adopted, except in some test cases to be described below; and mass loss has been ignored. In the earlier work, the TAMS stage was taken, for convenience, to occur when $X_c = 0.05$, but in the present work it has been located exactly. Results for the new stellar models are given in Table 1. These will be discussed below in conjunction with a parallel set of results to be derived for rotating and magnetic stellar models.

III. ROTATING STAR MODELS

Rotation has been introduced into the new stellar models by a simple device in which the only modification of the basic equations of spherical stellar structure is the addition of a mean centrifugal force, averaged over a spherical shell, to the gravitational force in the equation of hydrostatic equilibrium. This equation then reads:

$$\frac{dP}{dr} = -\frac{GM(r)\rho}{r^2}(1-\lambda)\,, \tag{2}$$

with

$$\lambda = \tfrac{2}{3}\Omega^2 r^3/GM(r)\,, \tag{3}$$

Ω being the angular velocity about the rotation axis (Monaghan 1968). In the present approximation, r is to be interpreted physically as the mean radius of the stellar surface.

Our main concern here will be with the case of *uniform* rotation, for three important reasons. First, the convective motions within the core and semiconvective zone are likely, because of turbulent viscosity, to maintain rigid rotation of these hydrodynamically connected regions, while the Eddington-Vogt circulation currents in the radiative envelope will probably penetrate the semiconvective zone, thereby coupling the envelope's rotation with the core's. (If a strong magnetic field is present, its rigidity would probably also help to maintain uniformity of rotation in the magnetic layers.) Second, it is known in the case of models of stars with lower masses that if these stars begin their evolution in a state of uniform rotation, they tend to preserve, in an approximate way, a state of uniform rotation to the end of the main-sequence phase of evolution, even if their available angular momentum is assumed to be redistributed according to different laws (Kippenhahn, Meyer-Hofmeister, and Thomas 1970; Endal and Sofia 1978). There is no reason to believe that models of more massive stars would evolve any differently. Third, a state of uniform rotation, or a fair approximation to it, is suggested by various kinds of observational data (see Stothers 1972, 1973; Hardorp 1974).

If, then, uniform rotation is a reasonable assumption, it will still be necessary to make other, less easily justifiable assumptions in order to construct actual stellar models. Thus, we assume that rotation has no significant effect on the Schwarzschild criterion for convection, or on the condition for convective neutrality, or on the actual occurrence of semiconvection, other than the formal inclusion of the factor $1 - \lambda$ in the quantity $\nabla_{\rm rad}$, since $\nabla_{\rm rad}$ is inversely proportional to dP/dr, which is given by equation (2). Although rotation leads to a number of instabilities on various time scales (see, e.g., Endal and

TABLE 2

UNIFORMLY ROTATING STAR MODELS (at breakup)

Stage	$M/M_\odot$	λ_R	v_e (km s^{-1})	$\log (L/L_\odot)$	$\log (R/R_\odot)$	$\log T_e$	$\log T_c$	$\log \rho_c$	β_c	$\rho_c/\langle\rho\rangle$	X_c
ZAMS.....	15	0.3007	632	4.225	0.738	4.451	7.506	0.746	0.902	43	0.739
	30	0.3007	741	5.012	0.901	4.566	7.558	0.507	0.788	39	0.739
	60	0.3007	867	5.655	1.066	4.644	7.598	0.318	0.647	39	0.739
	120	0.3007	1007	6.185	1.237	4.691	7.627	0.158	0.507	44	0.739
TAMS.....	15	0.3007	446	4.536	1.042	4.376	7.629	1.009	0.775	645	0.040
	30	0.3007	462	5.355	1.311	4.446	7.689	0.801	0.579	1286	0.026
	60	0.3007	494	5.939	1.554	4.471	7.729	0.645	0.419	2404	0.019
	120	0.3007	535	6.391	1.786	4.468	7.753	0.498	0.303	4261	0.018

Sofia 1978), the rate and extent of possible chemical mixing due to these instabilities are not known. But in any case the true gradient of hydrogen in the inhomogeneous zone is not expected to differ very much from the gradient based on equation (1).

The luminosity, radius, and effective temperature that are actually measured for a rotating star depend on the aspect angle. We shall follow a number of other authors in assigning a mean effective temperature to our stellar models based on the total emergent luminosity L and the mean radius R:

$$T_e = (L/4\pi\sigma R^2)^{1/4} . \quad (4)$$

Similarly, we define $\langle\rho\rangle = 3M/4\pi R^3$.

A last quantity of interest is the equatorial velocity of rotation, v_e. From the idealized Roche model, we adopt for the extreme case where centrifugal force balances gravity at the equator

$$v_e = 1.304R\Omega , \quad (5)$$

the quantity $1.304R$ being the critical equatorial radius (the polar radius is exactly $\frac{2}{3}$ of this value) (Sackmann and Anand 1970). Note that equation (3) provides the link between Ω and λ, which, for the Roche model at breakup, has a surface value of $\lambda_R = 0.3007$.

The adequacy of our methods to give numerically accurate results for massive, uniformly rotating ZAMS stars has been demonstrated elsewhere (Stothers 1974). Even at the breakup limit, the maximum error incurred in basic stellar quantities like luminosity and mean radius has been shown to be only about one part in 10^3. For the more centrally condensed TAMS models, the maximum error is expected to be even smaller, since the approximations involved in our approach are most suited to the infinitely condensed Roche model (cf. Faulkner, Roxburgh, and Strittmatter 1968; Sackmann and Anand 1970). Details of the present ZAMS and TAMS models are provided in Table 2.

Since the qualitative behavior of rotating models has been discussed by so many authors, we need not repeat this discussion here, but rather we turn immediately to a brief comparison of our results with those published by other authors. The comparison is shown in Table 3, where the most important physical input data, including opacity

TABLE 3

COMPARISON OF DIFFERENCES BETWEEN NONROTATING AND UNIFORMLY ROTATING (at breakup) STAR MODELS ON THE ZAMS

$M/M_\odot$	Opacity	X_e	Z_e	$\Delta L/L_0$ (%)	$\Delta R_p/R_{p0}$ (%)	Reference
15.....	Modified Kramers[a]	0.670	0.030	−6.5	−1.2	Sackmann and Anand 1970
15.....	Cox-Stewart	0.739	0.021	−7.7	−2.5	Sackmann 1970
15.....	Cox-Stewart	0.739	0.021	−7.9	−2.7	Present
20.....	Cox-Stewart	0.739	0.021	−7.5	−2.1	Sackmann 1970
20.....	Cox-Stewart[b]	0.739	0.021	−8.1	−2.5	Papaloizou and Whelan 1973
28.2.....	Thomson	[c]	[c]	−48.5[d]	...	Mark 1968
28.2.....	Cox-Stewart[b]	0.739	0.021	−8.0	−2.3	Papaloizou and Whelan 1973
30.....	Cox-Stewart	0.700	0.030	−8[d]	...	Jackson 1970*b*
30.....	Cox-Stewart	0.739	0.021	−7.7	−2.2	Present
40.....	Cox-Stewart[b]	0.739	0.021	−7.7	−1.9	Papaloizou and Whelan 1973
60.....	Cox-Stewart	0.739	0.021	−7.1	−0.9	Present
62.7.....	Thomson	[c]	[c]	−17.2	−11.6	Mark 1968
62.7.....	Thomson	0.750	0.030	−8.8	−2.4	Monaghan and Smart 1971
62.7.....	Cox-Stewart[b]	0.739	0.021	−7.3	−1.1	Papaloizou and Whelan 1973
120.....	Cox-Stewart	0.739	0.021	−6.2	+1.2	Present

[a] Formula provided by Larson (Morris and Demarque 1966).
[b] Fitted formula provided by Papaloizou (1973).
[c] Polytropic model.
[d] Extrapolated value.

TABLE 4

DIFFERENCES BETWEEN NONROTATING AND UNIFORMLY ROTATING (at breakup) STAR MODELS OF $15M_\odot$ ON THE ZAMS

Opacity	X_e	Z_e	$(\rho_c/\langle\rho\rangle)_0$	$\Delta L/L_0$ (%)	$\Delta R_p/R_{p0}$ (%)	$\Delta R/R_0$ (%)	$\Delta T_e/T_{e0}$ (%)
Thomson	0.739	0.021	20	−10.6	−3.6	+10.9	−7.7
Cox-Stewart	0.739	0.021	30	−7.9	−2.7	+11.9	−7.3
	0.650	0.021	30	−7.8	−2.5	+12.2	−7.5
	0.739	0.044	35	−7.3	−2.5	+12.2	−7.3
Modified Kramers[a]	0.739	0.021	37	−6.3	−1.3	+13.5	−7.7
Carson	0.739	0.021	43	−5.3	−0.6	+14.3	−7.7

[a] Formula provided by Larson (Morris and Demarque 1966).

and chemical composition, are also quoted. In this and other tables, $\Delta L/L_0$ refers to the relative change in luminosity between a nonrotating model (with luminosity L_0) and a model rotating at breakup velocity; the polar radius change $\Delta R_p/R_{p0}$ is defined analogously. Four models are discrepant. Mark's (1968) two polytropic models have been discussed fully by Whelan, Papaloizou, and Smith (1971) and by Papaloizou and Whelan (1973). The apparent discrepancies of Sackmann and Anand's (1970) and Monaghan and Smart's (1971) models are due to the opacities used, as will be demonstrated below. In addition, there are the simplified nondimensional models constructed by Sweet and Roy (1953), Roxburgh, Griffith, and Sweet (1965), Sanderson, Smith, and Hazlehurst (1970), Jackson (1970*a*), Jackson *et al.* (1971), and Smith (1973, 1977), which are not shown in Table 3.

In order to ascertain which single structural parameter is most important in controlling the luminosity changes, we have studied a number of special models, whose characteristics are given in Table 4, thereby forming a supplement to Table 2. The effects on the models of zero-age chemical composition, opacity, and evolution are included in these two tables. It is found that the most influential structural parameter is the central condensation. This quantity determines, in essence, how much of the star's mass feels the effect of uniform rotation, as can be understood by considering the simple rotational relation $\lambda_R/\lambda_c = \rho_c/\langle\rho\rangle$. With a large value of $\rho_c/\langle\rho\rangle$, the interior of the star rotates very slowly in comparison with the surface layers; accordingly the luminosity is hardly influenced. On the other hand, the amount of distortion of the surface layers depends almost exclusively on the properties of the outer part of the envelope (see Appendix); hence the percentage change in the surface radius is rather less sensitive to the star's central condensation.

In addition to the models rotating at breakup, we have computed several less-extreme models for the purpose of determining whether the drop in luminosity is approximately proportional to Ω^2, as has been found to be true for rotating models of lower mass (Faulkner, Roxburgh, and Strittmatter 1968; Kippenhahn and Thomas 1970; Sackmann and Anand 1970; Sackmann 1970). For convenience, we show in Figure 1 our results in terms of the alternate quantities λ_R and $\Delta \log (L/L_\odot)$, all for our standard physical assumptions. It is found that $\Delta \log (L/L_\odot)$ is roughly linear with λ_R and nearly independent of stellar mass. The same conclusion holds for $\Delta \log (R/R_\odot)$, as well as for $\Delta \log T_e$, which is shown in the lower panel of this figure.

Turning now to the TAMS models, we display a parallel set of results for $\Delta \log (L/L_\odot)$ and $\Delta \log T_e$ in Figure 2. Strictly speaking, the different models for a specified mass have slightly different hydrogen profiles depending on the assigned value of λ_R, because we have used equation (1) to determine the variable hydrogen abundance in the inhomogeneous zone and also because the TAMS stage does not correspond to a fixed value of the central hydrogen abundance. Supplementary calculations, however, indicate that this small compositional difference has a negligible effect on the results. Qualitatively the same behavior of $\Delta \log (L/L_\odot)$ and $\Delta \log T_e$ is found for the TAMS models as for the ZAMS models, but the drop in luminosity is now somewhat reduced on account of the large central condensation of the TAMS models (see also Hazlehurst and Thomas 1970). In compensation, the mean effective temperature decreases by a correspondingly larger amount. One further result is worth noting here: when the mean radius of the star exceeds $\sim 15\ R_\odot$, uniform rotation causes the *entire* surface of the star (including the poles) to expand.

The location of both the ZAMS and TAMS models on the H-R diagram is shown in Figure 3. If one may correctly judge from the evolutionary sequences published for models of stars of lower mass, the TAMS models at maximum rotation are not to be regarded, necessarily, as evolutionary derivatives of the fastest-rotating ZAMS models. It is sufficient that they have started out with modest initial velocities and simply have conserved their total angular momentum during evolution (Crampin and Hoyle 1960). Larger initial velocities will cause them to lose some mass, but the amount of matter ejected seems to be very small in all cases computed so far (Nobili and Secco 1969; Strittmatter, Robertson, and Faulkner 1970; Meyer-Hofmeister and Thomas 1970; Musylev, Tutukov, and Chevalier 1970; Gredley and Borra 1972). Therefore, we may safely regard the displaced TAMS line in Figure 3 as representing the maximum shift obtainable for stars that are rotating

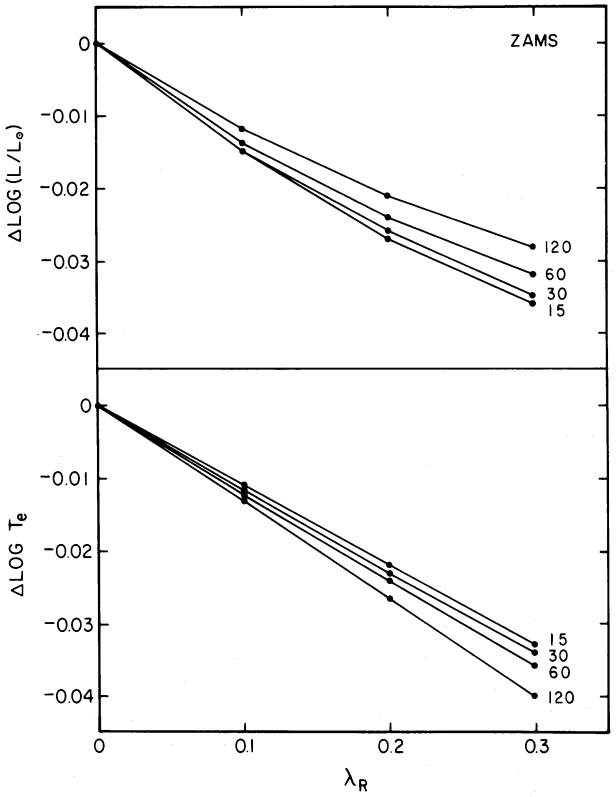

FIG. 1.—Differences in surface quantities between nonrotating and uniformly rotating star models on the ZAMS as a function of the surface rotation parameter λ_R. Stellar masses are indicated in solar units.

uniformly. Fortunately, both this line and the displaced ZAMS line can be compared directly with observations—even though these lines refer to *mean* stellar quantities—because the locations of lines like these in the H-R diagram are known to be virtually independent of aspect angle (e.g., Sweet and Roy 1953; Roxburgh and Strittmatter 1965; Faulkner, Roxburgh, and Strittmatter 1968).

IV. MAGNETIC STAR MODELS

Stellar magnetic fields probably have varying degrees of geometrical complexity, but we shall consider here the limiting case of a severely tangled interior magnetic field, which is probably appropriate to very massive stars. A field of this kind exerts an isotropic pressure of amount $\langle H^2 \rangle/24\pi$, where $\langle H^2 \rangle$ represents the mean square of the magnetic field intensity averaged over a spherical shell (Trasco 1970). To compute the relevant stellar models, it is sufficient to proceed in the same fashion as we did in the case of axial rotation by modifying the equation of hydrostatic equilibrium only. This equation is then written:

$$\frac{dP}{dr} = -\frac{GM(r)\rho}{r^2} - \frac{d}{dr}\left(\frac{\langle H^2 \rangle}{24\pi}\right). \tag{6}$$

A further simplification results from setting $\langle H^2 \rangle/24\pi \propto P^a$; then it follows that

$$\frac{dP}{dr} = -\frac{GM(r)\rho}{r^2}\left(\frac{1}{1+av}\right), \tag{7}$$

with

$$v = \langle H^2 \rangle/24\pi P\,. \tag{8}$$

For lack of a better alternative, the criterion for convection and the definition of semiconvection will be assumed to remain unchanged in the presence of the magnetic field, except insofar as $\nabla_{\rm rad}$ is changed by the use of equation (7). Chemical mixing due to magnetically caused instabilities will also be ignored. In any case, we are concerned here only with small (though not negligible) values of v.

Three spatial distributions of the magnetic field intensity will be considered for illustration: (1) a uniform mean field intensity; (2) a nonuniform mean field intensity with v = constant everywhere; and (3) the same as case (2), but with no magnetic field allowed in the convective core.

The first case, in which $\langle H^2 \rangle$ is constant everywhere, leads to a state of hydrostatic equilibrium which is identical to that for the nonmagnetic case, as a glance at equation (6) reveals. Therefore, the stellar models of Table 1 apply also to the present case, regardless of how large an intensity of the magnetic field is assumed.

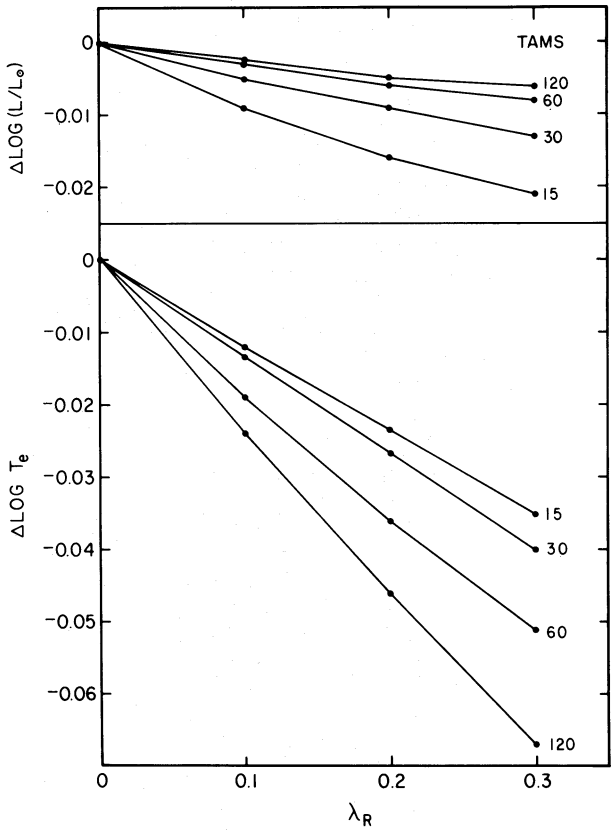

FIG. 2.—Differences in surface quantities between nonrotating and uniformly rotating star models on the TAMS as a function of the surface rotation parameter λ_R. Stellar masses are indicated in solar units.

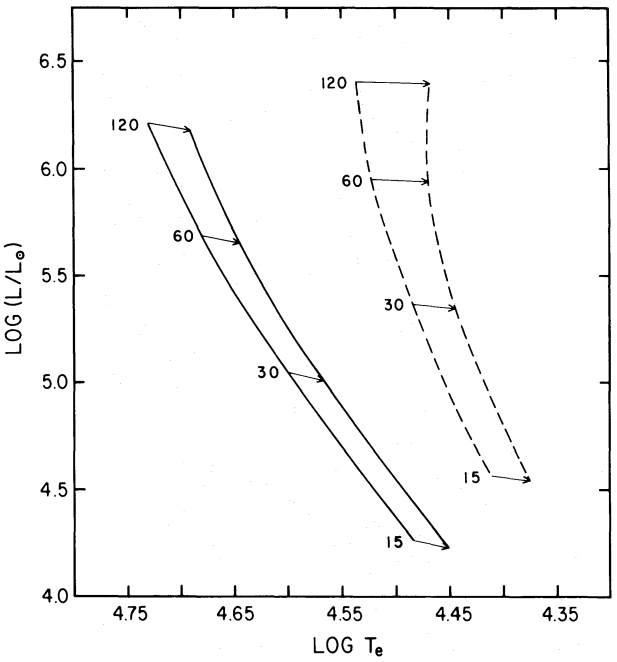

FIG. 3.—Theoretical H-R diagram showing the ZAMS (*solid curves*) and TAMS (*dashed curves*) for both nonrotating and uniformly rotating (at breakup) star models. Stellar masses are indicated in solar units.

In the second case, a strong magnetic field has a large effect on the models, since the ratio of total magnetic energy to total gravitational potential energy is now quite significant (it is completely negligible in the first case for any reasonable surface field) (Stothers 1979). Because the magnetic stresses support much of the weight of the star, the average thermodynamic pressures, and hence the average temperatures, are lower; therefore the luminosity decreases. This argument can be made more quantitative by noticing that with v constant the basic equations admit a crude similarity solution, consisting of $L \sim (1 + v)^{-4}$, and $R \sim (1 + v)^{-0.6}$. It is clear that the radius, together with the central condensation, has only a marginal dependence on v; but the relatively strong dependence of the luminosity on v enables us to place a stringent limit of $v < 0.2$ on the possible magnetic field strength in upper main-sequence stars, by considering the dispersion of the observed mass-luminosity relation. As a practical upper limit, however, we shall adopt $v = 0.11$. This corresponds, in the photosphere of the star, to a rms magnetic field strength of several hundred gauss. Stellar models based on this limit are presented in Tables 5 and 6. The numerical results support the simple predictions of the similarity solution, including the prediction that the size of the luminosity and radius changes should be essentially independent of the star's central condensation.

When v is set equal to zero in the convective core, we obtain the third of our assumed distributions of the stellar magnetic field. This case allows for the possibility that turbulent convection, though it may, in conjunction with rotation, generate a *small* magnetic field, may also dissipate or expel any preexisting *large* magnetic field. Stellar models corresponding to this case are listed in Table 5. In the models of highest mass, where the convective cores are very large, the perturbing effects of the magnetic field are concentrated relatively near the surface; therefore the radii are changed by a larger amount than are the luminosities. In the limit of very small stellar masses, the situation reverts to the case discussed in the preceding paragraph.

Vector displacements of all the magnetic models of Table 5 are shown on the H-R diagram in Figure 4. Although the displacements of the individual models are large, they do not result in significant shifts of the ZAMS and TAMS lines as a whole in the case where v is constant throughout the star. But if the magnetic field is concentrated mostly in the stellar envelope, the ZAMS and (though not explicitly shown) TAMS lines become shifted noticeably toward lower effective temperatures. This resulting pattern of shifts enables us to understand the displacements toward higher effective temperatures displayed by some of the models of Tutukov and Ruben (1974), because these previous models have *more centrally* concentrated magnetic fields than have ours.

The shifts exhibited by the magnetic models are reminiscent of the shifts obtained for rotating models with

TABLE 5

MAGNETIC STAR MODELS

Stage		Envelope v	Core v	log $(L/L_\odot)$	log $(R/R_\odot)$	log T_e	log T_c	log ρ_c	β_c	$\rho_c/\langle\rho\rangle$	X_c
ZAMS.....	15	0.11	0.11	4.083	0.677	4.445	7.492	0.790	0.918	31	0.739
	15	0.11	0	4.159	0.734	4.436	7.502	0.773	0.910	45	0.739
	30	0.11	0.11	4.903	0.840	4.569	7.547	0.539	0.811	27	0.739
	30	0.11	0	4.989	0.904	4.558	7.557	0.519	0.794	40	0.739
	60	0.11	0.11	5.575	0.999	4.657	7.589	0.342	0.672	26	0.739
	60	0.11	0	5.660	1.072	4.642	7.598	0.322	0.647	41	0.739
	120	0.11	0.11	6.124	1.160	4.714	7.621	0.179	0.531	27	0.739
	120	0.11	0	6.201	1.243	4.692	7.629	0.158	0.505	46	0.739
TAMS.....	15	0.11	0.11	4.358	0.948	4.379	7.605	1.037	0.815	358	0.051
	30	0.11	0.11	5.228	1.207	4.467	7.673	0.822	0.620	657	0.031
	60	0.11	0.11	5.853	1.435	4.509	7.721	0.674	0.448	1126	0.019
	120	0.11	0.11	6.325	1.639	4.525	7.750	0.535	0.324	1671	0.015

TABLE 6
DIFFERENCES BETWEEN NONMAGNETIC AND STRONGLY MAGNETIC ($v = 0.11$) STAR MODELS OF 15 $M_\odot$ ON THE ZAMS

Opacity	X_e	Z_e	$(\rho_c/\langle\rho\rangle)_0$	$\Delta L/L_0$ (%)	$\Delta R/R_0$ (%)	$\Delta T_e/T_{e0}$ (%)
Thomson	0.739	0.021	20	−31.1	−4.1	−7.1
Cox-Stewart	0.739	0.021	30	−33.6	−2.7	−8.6
	0.650	0.021	30	−32.5	−2.5	−8.2
	0.739	0.044	35	−35.3	−2.5	−9.0
Modified Kramers[a]	0.739	0.021	37	−34.1	−2.9	−8.6
Carson	0.739	0.021	43	−34.4	−4.1	−8.0

[a] Formula provided by Larson (Morris and Demarque 1966).

differing central concentrations of angular momentum (Mark 1968; Bodenheimer 1971; Monaghan and Smart 1971). The resemblance is more than merely coincidental, since a comparison of equations (2) and (7) reveals the identity $(1 - \lambda) = (1 + av)^{-1}$. For this reason, a comparison of Figures 3 and 4 can be taken as affording a comparison between uniformly rotating models (with $\lambda_R = 0.3007$) and nonuniformly rotating models (with $\lambda = 0.1$), provided that the rotational distortion of the star's inner regions can be neglected.

V. CONCLUSION

The present numerical calculations suggest that the largest possible displacements of the upper-main-sequence band in the H-R diagram due to axial rotation and tangled magnetic fields are likely to arise when the rotation is approximately uniform and the magnetic fields are concentrated in the outer part of the envelope. A simple analytic calculation (see Appendix) demonstrates that the region of the star which has the most weight in determining the surface radius is located in the outer part of the envelope around a radius fraction of $r/R = 0.5$. Unfortunately, it is not known how rotation and magnetic fields interact with each other in a real star. But we have at least verified by a few additional numerical calculations that the vector displacements in the H-R diagram due to each of the two perturbations treated separately are linearly additive, to a close approximation, if one wishes to obtain the combined displacement due to both perturbations acting together. Furthermore, the sizes of the displacements are found to be proportional to λ_R and to v, to a good approximation.

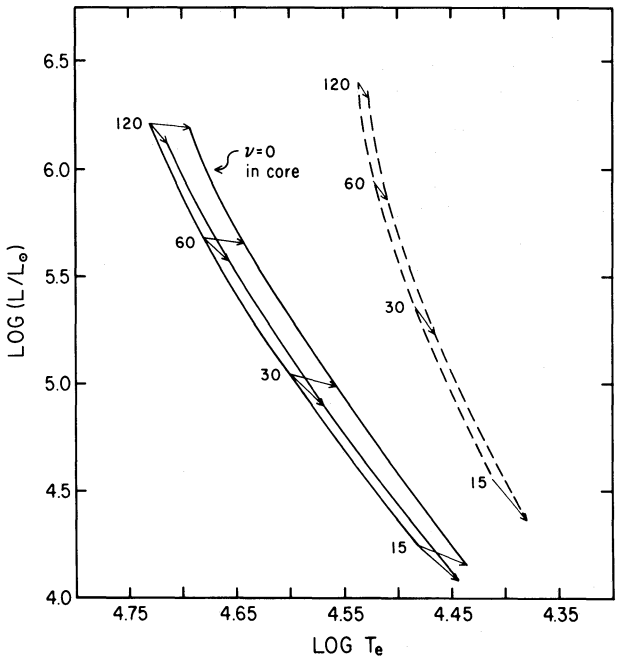

FIG. 4.—Theoretical H-R diagram showing the ZAMS (*solid curves*) and TAMS (*dashed curves*) for both nonmagnetic and strongly magnetic ($v = 0.11$) star models. The ZAMS for magnetic models with $v = 0$ in the convective core is also shown. Stellar masses are indicated in solar units.

In a random sample of real stars, there will inevitably be some intrinsic dispersion of the rotational velocities and magnetic fields. Except for the unlikely case in which an unevolved star has a greatly perturbed central region, the hot edge of the main-sequence band in the H-R diagram should correspond to the most slowly rotating, least-magnetic ZAMS stars. By the same reasoning, the cool edge should refer to the TAMS stars with the largest radial distortions. It is therefore interesting to observe that for luminosities greater than $\log (L/L_\odot) = 4.5$ there appears to be *no* determinable cool edge; the brightest main-sequence stars just merge into the supergiants.

This fact cannot be explained by the present calculations. Rotation and magnetic fields, together, can displace the cool edge by at most $\delta \log T_e \approx 0.08$ (rotation alone causes a shift of less than $\delta \log T_e \approx 0.04$). The present models therefore cannot close the gap of at least $\delta \log T_e \approx 0.15$ that separates the reddest nonrotating, nonmagnetic models burning core hydrogen from the bluest nonrotating, nonmagnetic models burning core helium, in stages of evolution that slow enough to be readily observable (Stothers and Chin 1976). As far as rotation and magnetic fields are concerned, it is most unlikely that the incorporation of these effects could make the helium-burning models any bluer. Therefore, we conclude that the observed distribution of early-type stars in the H-R diagram probably requires a theoretical explanation along some entirely different line.

APPENDIX

INFLUENCE OF OPACITY AND ROTATION ON THE STELLAR RADIUS

A simple analytic treatment will be given here of the way in which opacity and rotation in the outer layers of the stellar envelope affect the total radius of a massive star. The region of the star in question will be assumed to be in radiative equilibrium, and the luminosity L, the mass M, and the ratio of radiation pressure to total pressure $1 - \beta$ will be taken to be constant there.

If the opacity coefficient is represented approximately by the formula $\kappa = \kappa_0 \rho^{\alpha} T^{-\eta}$, α and η being constants, the local effective polytropic index can easily be shown to be

$$n = (3 + \eta)/(1 + \alpha)\,, \tag{A1}$$

in the absence of rotation (Cox and Giuli 1968, eq. [20.33]). Now, in all realistic cases, the hot inner part of the envelope is dominated by electron-scattering opacity, so that any change, let us specify an increase, in the uncertain low-temperature opacities will also affect (here increase) η. It then follows that n too will increase; consequently, according to simple polytrope theory (e.g., Cox and Giuli 1968, Table 23.1), the central condensation of the star will grow, and this implies a larger stellar radius.

To determine which layers in the envelope are most effective in changing the radius, we formally integrate the equation of radiative equilibrium:

$$R - r^* = \int_{\ln T_e}^{\ln T^*} \frac{1}{\kappa}\left[\frac{16\pi ck(1-\beta)}{\mu\beta m_p L}\right] r^2 T d \ln T\,, \tag{A2}$$

r^* being the location of the base of the envelope. (In very centrally condensed models, $r^* \ll R$, and it is valid to ignore r^* entirely.) The term appearing in brackets in equation (A2) can, by virtue of our initial approximations, be assumed to be constant. Moreover, we have chosen $\ln T$ as the independent variable because its range is (to within a few percent) independent of the particular model; specifically, $\ln T^* - \ln T_e \approx 7$. Therefore, the problem reduces to determining where $r^2 T$ has its maximum. For T we use the following integral of the equation of hydrostatic equilibrium:

$$T = \frac{\mu\beta m_p GM}{k(n+1)}\left(\frac{1}{r} - \frac{1}{R}\right) \tag{A3}$$

(Cox and Giuli 1968, eq. [20.115]). It then easily follows that $r^2 T$ is largest at $r/R = 0.5$.

At this layer in actual stellar models, we find $M(r)/M = 0.90 \pm 0.05$, thus confirming our initial assumption that $M(r) \approx M$. Furthermore, the temperature at this layer is found to be $\log T = 6.9 \pm 0.2$. Consequently, our results agree well with those of Parsian, Refsdal, and Stabell (1974), who integrated a series of stellar models for 15 $M_\odot$ in which arbitrary opacity changes were made in different layers of the star, yielding a peak effect near $\log T = 7.0$. But our results are evidently more general than theirs, provided of course that none of our initial assumptions is violated. It should be noted that the function $r^2 T$ varies rather slowly around its maximum value, and therefore is still of substantial size at temperatures of $\log T = 5.5$–6.5, where the subsurface opacities are most uncertain. The resulting effect on the stellar radius (i.e., on $\rho_c/\langle\rho\rangle$) can be seen in the sequence of nonrotating models for 15 $M_\odot$ in Table 4, where four different opacity representations are listed in order of increasing size of the low-temperature contribution to the opacities.

Next we turn to the effect caused by uniform rotation. Let the run of the rotation parameter $1 - \lambda$ be approximated by CP^{ζ}, where P is the pressure and ζ and C are constants. Then the local effective polytropic index becomes

$$n = (3 + \eta + \zeta)/(1 + \alpha - \zeta)\,. \tag{A4}$$

Since $1 - \lambda$ increases inward from the surface, ζ must be positive. Hence uniform rotation increases n and, consequently, R. To determine the most effective layers for increasing the radius, we formally integrate the equation of hydrostatic equilibrium:

$$R - r^* = \int_{\ln T_e}^{\ln T^*} \frac{1}{1-\lambda}\left[\frac{k(n+1)}{\mu\beta m_p GM}\right] r^2 T d \ln T\,. \tag{A5}$$

Again, the weighting function is seen to be $r^2 T$; but for T we must now use

$$T = \frac{\mu\beta m_p GM}{k(n+1)}\left[\left(\frac{1}{r} - \frac{1}{R}\right) - \frac{\lambda_R}{2R^3}(R^2 - r^2)\right], \tag{A6}$$

where we have employed the approximation $\lambda = \lambda_R (r/R)^3$, which is certainly valid in the outer part of the envelope. The

new maximum of r^2T will occur at a value of r/R that is determined from the solution of the cubic equation

$$2\lambda_R(r/R)^3 - (2 + \lambda_R)(r/R) + 1 = 0 \,. \tag{A7}$$

In the limit of maximum rotation (i.e., at equatorial breakup), $r/R = 0.46$, whereas in the limit of very slow rotation, $r/R = 0.50$.

Even if the rotation law is not that of uniform rotation but Ω increases inward as $r^{-3/2}$ (i.e., λ is approximately constant), a value of $r/R = 0.50$ is obtained. More generally, any perturbing force that can be formally represented as a constant multiple of the local gravitational force will have its greatest effect on the stellar radius at $r/R = 0.50$.

REFERENCES

Andrews, P. J. 1968, *Mem. R.A.S.*, **72**, 35.
Balona, L. A. 1975, *M.N.R.A.S.*, **173**, 449.
Bodenheimer, P. 1971, *Ap. J.*, **167**, 153.
Bodenheimer, P., and Ostriker, J. P. 1970, *Ap. J.*, **161**, 1101.
Clement, M. J. 1979, *Ap. J.*, **230**, 230.
Conti, P. S., and Ebbets, D. 1977, *Ap. J.*, **213**, 438.
Cox, J. P., and Giuli, R. T. 1968, *Principles of Stellar Structure* (New York: Gordon and Breach).
Crampin, J., and Hoyle, F. 1960, *M.N.R.A.S.*, **120**, 33.
Dudorov, A. E. 1974, *Nauch. Inform.*, **29**, 80.
Ebbets, D. 1979, *Ap. J.*, **227**, 510.
Endal, A. S., and Sofia, S. 1976, *Ap. J.*, **210**, 184.
———. 1978, *Ap. J.*, **220**, 279.
———. 1979, *Ap. J.*, **232**, 531.
Faulkner, J., Roxburgh, I. W., and Strittmatter, P. A. 1968, *Ap. J.*, **151**, 203.
Gredley, P. R., and Borra, E. F. 1972, *Ap. J.*, **172**, 609.
Hardorp, J. 1974, *Astr. Ap.*, **32**, 133.
Harris, W. E., and Clement, M. J. 1971, *Ap. J.*, **167**, 321.
Hazlehurst, J., and Thomas, H. C. 1970, *M.N.R.A.S.*, **150**, 311.
Humphreys, R. M., and Davidson, K. 1979, *Ap. J.*, **232**, 409.
Jackson, S. 1970*a*, *Ap. J.*, **160**, 685.
———. 1970*b*, *Ap. J.*, **161**, 579.
Jackson, S., Sanderson, A. D., Smith, R. C., and Hazlehurst, J. 1971, *Ap. J.*, **165**, 223.
Kippenhahn, R., Meyer-Hofmeister, E., and Thomas, H. C. 1970, *Astr. Ap.*, **5**, 155.
Kippenhahn, R., and Thomas, H. C. 1970, in *Stellar Rotation*, ed. A. Slettebak (Dordrecht: Reidel), p. 20.
Kopylov, I. M. 1959, *Ann. d' Ap. Suppl.*, **8**, 41.
Mark, J. W.-K. 1968, *Ap. J.*, **154**, 627.
Meyer-Hofmeister, E. 1972, *Astr. Ap.*, **16**, 282.
Meyer-Hofmeister, E., and Thomas, H. C. 1970, *Astr. Ap.*, **5**, 490.
Monaghan, J. J. 1968, *Zs. Ap.*, **68**, 461.
Monaghan, J. J., and Smart, N. C. 1971, *M.N.R.A.S.*, **153**, 195.
Morris, S. C., and Demarque, P. 1966, *Zs. Ap.*, **64**, 238.
Musylev, V. 1972, *Nauch. Infor.*, **21**, 11.
Musylev, V., Tutukov, A. V., and Chevalier, C. 1970, *Nauch. Infor.*, **16**, 48.
Nobili, L., and Secco, L. 1969, in *Mass Loss from Stars*, ed. M. Hack (Dordrecht: Reidel), p. 135.
Papaloizou, J. C. B. 1973, *M.N.R.A.S.*, **162**, 143.
Papaloizou, J. C. B., and Whelan, J. A. J. 1973, *M.N.R.A.S.*, **164**, 1.
Parsian, I., Refsdal, S., and Stabell, R. 1974, *Astr. Ap.*, **30**, 275.
Roxburgh, I. W., Griffith, J. S., and Sweet, P. A. 1965, *Zs. Ap.*, **61**, 203.
Roxburgh, I. W., and Strittmatter, P. A. 1965, *Zs. Ap.*, **63**, 15.
Sackmann, I.-J. 1970, *Astr. Ap.*, **8**, 76.
Sackmann, I.J., and Anand, S. P. S., 1970, *Ap. J.*, **162**, 105.
Sanderson, A. D., Smith, R. C., and Hazlehurst, J. 1970, *Ap. J. (Letters)*, **159**, L69.
Schlesinger, B. M. 1975, *Ap. J.*, **199**, 166.
Schwarzschild, M., and Härm, R. 1958, *Ap. J.*, **128**, 348.
Slettebak, A. 1956, *Ap. J.*, **124**, 173.
Smith, B. L. 1973, *Ap. Space Sci.*, **25**, 195.
———. 1977, *Ap. Space Sci.*, **47**, 61.
Stothers, R. 1972, *Ap. J.*, **175**, 431.
———. 1973, *Ap. J.*, **184**, 181.
———. 1974, *Ap. J.*, **192**, 145.
———. 1979, *Ap. J.*, **229**, 1023.
Stothers, R., and Chin, C.-w. 1976, *Ap. J.*, **204**, 472.
Strittmatter, P. A., Robertson, J. W., and Faulkner, D. J. 1970, *Astr. Ap.*, **5**, 426.
Sweet, P. A., and Roy, A. E. 1953, *M.N.R.A.S.*, **113**, 701.
Trasco, J. D. 1970, *Ap. J.*, **161**, 633.
Tuominen, I., and Musylev, V. 1974, *Nauch. Infor.*, **33**, 48.
Tutukov, A. V., and Ruben, G. V. 1974, *Nauch. Infor.*, **31**, 5.
Whelan, J. A. J., Papaloizou, J. C. B., and Smith, R. C. 1971, *M.N.R.A.S.*, **152**, 9P.

R. STOTHERS: NASA Institute for Space Studies, Goddard Space Flight Center, 2880 Broadway, New York, NY 10025